

## **MULTISPECTRAL AIRBORNE LASER SCANNING - A NEW TREND IN THE DEVELOPMENT OF LIDAR TECHNOLOGY**

## **MULTISPEKTRALNE LOTNICZE SKANOWANIE LASEROWE - NOWY TREND W ROZWOJU TECHNOLOGII LIDAR**

**Krzysztof Bakula**

Warsaw University of Technology, Faculty of Geodesy and Cartography  
Department of Photogrammetry, Remote Sensing and Spatial Information Systems

**KEY WORDS:** multispectral laser scanning, multi-wavelength ALS, LiDAR technology development, classification, colour composite, land cover map

**ABSTRACT:** Airborne laser scanning (ALS) is the one of the most accurate remote sensing techniques for data acquisition where the terrain and its coverage is concerned. Modern scanners have been able to scan in two or more channels (frequencies of the laser) recently. This gives the rise to the possibility of obtaining diverse information about an area with the different spectral properties of objects. The paper presents an example of a multispectral ALS system - Titan by Optech - with the possibility of data including the analysis of digital elevation models accuracy and data density. As a result of the study, the high relative accuracy of LiDAR acquisition in three spectral bands was proven. The mean differences between digital terrain models (DTMs) were less than 0.03 m. The data density analysis showed the influence of the laser wavelength. The points clouds that were tested had average densities of 25, 23 and 20 points per square metre respectively for green (G), near-infrared (NIR) and shortwave-infrared (SWIR) lasers. In this paper, the possibility of the generation of colour composites using orthoimages of laser intensity reflectance and its classification capabilities using data from airborne multispectral laser scanning for land cover mapping are also discussed and compared with conventional photogrammetric techniques.

### **1. INTRODUCTION**

Airborne laser scanning (ALS) is the one of the most accurate remote sensing data acquisition technologies. It has become a source of data for researchers and professionals in many fields of the natural, technical and human sciences. For the long-term development of laser scanners over the years, the highest possible accuracy for measurement and the highest density of data have been expected. This has been related to the acquisition of data of good quality at the lowest cost possible. Currently, there are several opportunities for the further development of LiDAR systems, among which the range increment and registration in several spectral bands can be mentioned here. The latest trend in the development of LiDAR technology considers a different approach to ALS point clouds that can create land cover maps more effectively than typical topographic ALS.

In the development of ALS technology, an important step has been the appearance of airborne hydrographic scanners (bathymetric scanner) due to the fact that the near-infrared (NIR) laser in topographic scanners is completely absorbed by water. This sensor has enabled the collection of data in shallow-water areas. In various manufacturer's solutions, a laser at a frequency corresponding to the range of green (G) light was used. When the intensity images taken in the same area from scanning systems with lasers of various wavelengths were analysed, different reflective properties of objects were noticed. These results could be interpreted as passive multispectral data. Today, airborne laser hydrography scanners working in both G and NIR lasers are used. The selected bathymetric airborne laser systems are presented in Table 1. In addition to the typical bathymetric scanner, there are two additional sensors listed in this table that register in more than two spectral bands: Leica Hawk Eye III and Titan, by Optech. The Leica sensor scans with three channels but only in two wavelengths. The registration in the G band is conducted with two different laser settings (the scan rate and power) which allow for the penetration of a body of water at different depths. This scanner is a very powerful tool dedicated to bathymetric measurements. On the other hand, additional acquisition in the G band is less useful for topographic scanning. The results from two G channels would be comparable in non-forested areas, which may greatly limit using information from the same spectral band. Titan, by Optech, released in 2014, operates simultaneously with three spectral bands: two NIR (1064 nm and 1550 nm) and G (532 nm) lasers providing for the possibility of surveying 3D data but also obtaining spectral information about scanned objects in independent channels.

Table 1. Selected bathymetric and multispectral airborne laser scanners  
(source: Doneus *et al.*, 2015 with modifications).

Scanner	Wavelength	Scan rate	Depth range [Secchi]
Optech Aquarius	532 nm	70 kHz	1,0
Optech CZMIL	532 nm	70 kHz (10 kHz)	3,0
Riegl LMS VQ-820-G	532 nm	200 kHz 200 kHz	1,5
Riegl LMS VQ-880-G	532 nm	550 kHz	1,5
Leica Chiroptera II	1064 nm 532 nm	500 kHz 35 kHz	- 1,0
Optech Titan	1550 nm 1064 nm 532 nm	15-300 kHz 15-300 kHz 15-300 kHz	- - 1,0
Leica Hawk Eye III	1064 nm 532 nm 532 nm	500 Hz 35 kHz 10 kHz	- 1,5 3,0

To begin the discussion about the use of data from multispectral ALS, the use of LiDAR reflectance intensity should be mentioned because, beyond the typical uses of data from airborne scanners providing a dense and accurate georeferenced point cloud, it is the intensity that plays a crucial role in this kind of sensor. The LiDAR intensity is acquired as the amount of energy backscattered from objects using a laser beam. It depends on many factors, e.g., the distance to the object (energy loss), the local incidence angle between the laser beam and the footprint surface, the atmospheric influence, the laser transmission pulse energy, and the laser optics and receiver characteristics. The intensity registered with ALS systems can be useful for several applications, e.g., automatic point classification, LiDAR geo-reference, change detection and environmental studies. Before the intensity values can be used for any specific application, the system has to be calibrated. Some ALS systems use automatic gain controls (special targets) to calibrate ALS intensity data (Vain *et al.*, 2010). Another option is to use naturally available reference targets (Vain *et al.*, 2009). The intensity of the laser beam reflection is still less frequently used than the 3D information provided by LiDAR technology. Nevertheless, in the literature, many applications of intensity images can be found. Bare-earth and forested surfaces can be classified from the LiDAR intensity to determine ground elevations from LiDAR data according to the land cover information (Wang and Glenn, 2009). Intensity data can be used to map coastal habitats when it is integrated with altimetry data, topographically-derived features (the slope and aspect) and multi-spectral imagery (Chust *et al.*, 2008). This procedure has improved overall habitats classification accuracy - gains of up to 7.9% in mean producer's accuracy and 11.6% in the mean user's accuracy were observed (with an overall accuracy of 92% for the 16 rocky habitats and 88% for the 11 wetland habitats). Comparable results were noticed for forested wetlands in Lang and McCarty's investigation (2009), with over 96% overall accuracy. This demonstrates the strong potential of LiDAR intensity data for such an application. The ability of LiDAR intensity data for forest inundation mapping was compared with what is currently the most commonly used method for wetland mapping - false colour NIR aerial photography - where only 70% overall accuracy was achieved.

Multispectral LiDAR technology (MSL) was initially developed in laboratory experiments. Many studies have used terrestrial laser scanning systems for vegetation analysis, e.g., to define forests' structural and biochemical parameters from multispectral LiDAR (Wallace *et al.*, 2012), to classify data with the use of multispectral intensity reflectance after a calibration procedure based on the spectral ratio with vegetation indexes (Gong *et al.*, 2015). In this experiment, MSL was able to achieve an overall accuracy of 88.7%, which was 9.8-39.2% higher than that obtained using a single-wavelength LiDAR, and 4.2% higher than the use of multispectral images. Similar studies have also been conducted in relation to the testing capabilities and use of hyperspectral LiDAR scanning systems (i.e., Suomalainen *et al.*, 2011). In practice, such systems have not been used to collect aerial data. In contrast, the multispectral ALS technique is already possible and has been applied, as shown in Table 1.

Nowadays, even ultra-light scanners for unmanned aerial vehicles (Mierczyk *et al.*, 2013) have been constructed, but until multispectral airborne laser scanners were developed the issue of using multi-wavelength ALS had also been a subject of investigation. Pfennigbauer and Ullrich (2011) proposed the use of datasets from three single airborne scanners scanning at different wavelengths: Riegl LMS-Q680i (1550 nm), Riegl VQ-580 (1064 nm) and Riegl VQ 820-G (532 nm). The authors indicated that multispectral ALS

can provide data on targets in areas which cannot be measured at a single wavelength (low reflectance at some wavelengths) but which might be bright at other wavelengths. This gives additional information about the reflectance properties when the response in one wavelength is insufficient to identify a particular target. The application of such an approach can be found in investigations related to forestry (Morsdorf *et al.*, 2009) or to archaeology (Briese *et al.*, 2013).

The analysis of multispectral laser channels is the key topic of this article. In Fig. 1, it can be seen that the selection of channels for lasers used in ALS systems is related to the spectral characteristics of objects. Vegetation is strongly reflective in the NIR spectrum, and slightly so in the visible G spectrum. It is worth noting that, during penetration through vegetation, the LiDAR intensity decreases: the echo number is higher and the intensity value is lower. This makes it more difficult and completely alters the interpretation of vegetation on the intensity image with respect to classic composites from optical images of a passive sensor (aerial and satellite images with NIR registration). If the spectral reflectance is obtained with a few laser wavelengths, vegetation can be easily distinguished from soil and water (e.g., vegetation and non-vegetation). It can also be carried out with registration in the shortwave infrared (SWIR) channel. Due to the fact that electromagnetic waves are mostly absorbed at the water's surface in the NIR wavelength, water is best penetrated using the G channel. Three scanning frequencies make it possible to obtain various spectral responses and thus gain diverse information about land cover.

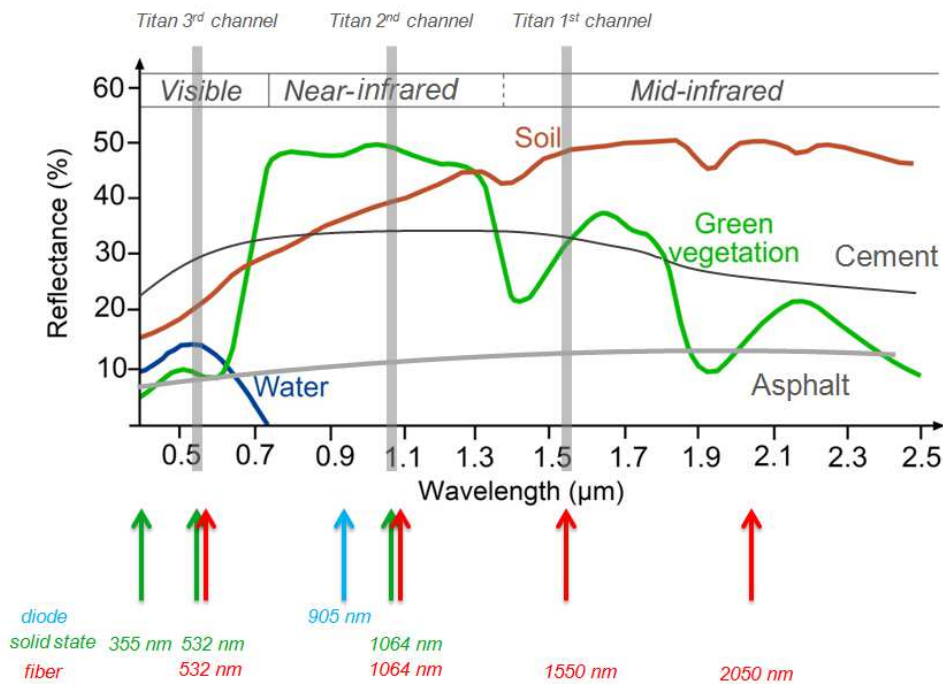


Fig. 1. Titan laser channels with spectral signatures for selected objects and available laser wavelengths for long-range ALS systems (based on Pfennigbauer and Ullrich (2011) with modifications).

The selection of a channel in passive multispectral sensors is much simpler because it is not limited by the construction of laser emitter. There are only a couple of wavelengths where the laser is powerful enough to be used in airborne scanners (Pfennigbauer and Ullrich, 2011). In the past, a diode laser at 905 nm was used in practice. Nowadays, the most popular wavelengths are 1064 nm, obtained with a solid state or fibre laser, and 1550 nm, obtained by a fibre laser. Additionally, it is possible to use other wavelengths with frequency-doubling, e.g., 532 nm used in airborne hydrographic scanners (Doneus *et al.*, 2015) and even with frequency tripling (Elsayed *et al.*, 2002). However, the UV wavelength has still not been used in the ALS technique. The number of frequencies is not limited and can be used with active fibres with different dopants: thulium (1470 nm), praseodymium (1300 nm) and holmium (2000 nm). There are many laser wavelengths but only a few can be used in airborne scanners (Fig. 1).

The first commercial ALS system combining three laser wavelengths began a discussion about the application of this type of data in land cover mapping. The aim of this paper is to discuss the properties of the Titan (by Optech) scanner, to show the potential of data collected with this sensor and to raise the question as to whether it can be an alternative for photogrammetric-based data sources. In the paper, initial data were tested for relative vertical accuracy assessment, density analyses, and the correlation between laser beam intensity images. In the paper, test data were processed for products such as digital elevation models and colour composites, and aspects of their visualization are discussed.



Fig. 2. The Titan system by Optech – the scanner and processing unit (<http://www.teledyneoptech.com>).

## 2. DATA TESTED

In the presented analysis, testing data provided by Optech along with the Titan scanner system (Fig. 2) were used. The data were measured in three independent scanning systems - namely active imaging channels that support 532 nm, 1064 nm and 1550 nm wavelengths. The G laser (the third Titan channel) captures data in a 7° forward tilt to map shallow water more effectively with a depth penetration of over 15 m possible in coastal waters. The

second channel (NIR) scans with a laser 0° nadir-looking and the first channel (SWIR) with 3.5° forward-looking. The scanning system allows the capturing of data from altitudes of 300-2000 m for IR laser wavelengths and 300-600 m for the G laser. The tested data were collected from 400 m with a pulse repetition frequency (PRF) of 600 kHz for the whole system (200 kHz for each scanning channel). The Titan system allows for a scan rate of up to 900 kHz (up to 300 kHz for each channel). The Titan can acquire data with angles of up to 60°. The analysed data were scanned with a maximum angle of 30°.

The data were collected in 2014 for the area of West Rouge, Toronto, Ontario, Canada. It is a suburban area along the shoreline of Lake Ontario, with mixed buildings and vegetation. The data were also collected over an area of lake water with different bottom - types in shallow water and characteristic harbours. Fig. 3 presents the described test area in an optical image (RGB) and three intensities of laser reflectance rasters registered with wavelengths of 532 nm, 1064 nm and 1550 nm. The scanning data were saved in separated files for three strips. Each strip consisted of three different LAS files for three channels saved according to the ASPRS standard. The LiDAR data were classified by the Terrasolid software automatically with manual correction, referring particularly to the ground, buildings and manually reclassified water surface.

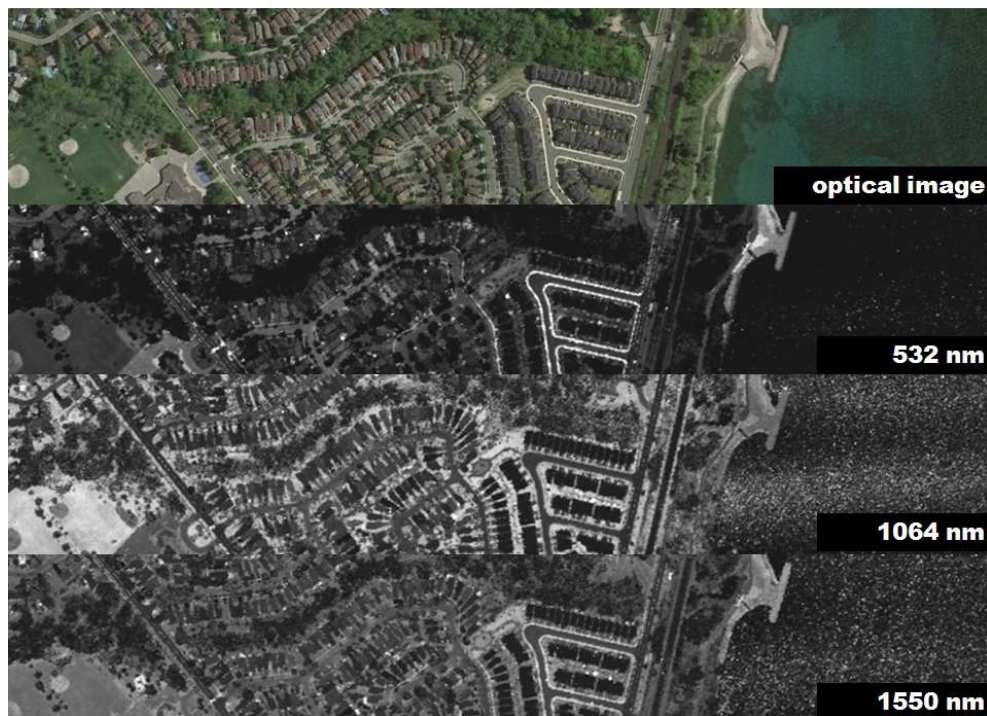


Fig. 3. The data tested: orthoimage and three laser intensity rasters for West Rouge, Ontario, Canada, acquired by the Titan scanner.



### 3. THE POSSIBILITY OF MULTISPECTRAL ALS-DERIVED PRODUCTS

Data from multispectral ALS provides more information than typical ALS. Beyond the three-dimensional information being the greatest benefit of the LiDAR technique, datasets containing information about the intensity of the laser reflection are provided. In practice, the intensity of reflection is not as commonly used as solely LiDAR-based point clouds, which can be a source for elevation models and 3D models. The acquisition of point clouds in at least three spectral bands allows for the collection of data containing point coordinates with other attributes in accordance with the ASPRS standard. Moreover, in addition to providing a minimum of three intensity reflectance values, multispectral ALS data can create colour composites from orthogonalized point clouds from the intensity image.

This chapter presents the results of the processing and analysis of data from multispectral laser scanning, whereby the properties of the point clouds and their relative accuracy and cohesion will be examined. The potential use of the laser intensity with three spectral bands will also be considered along with a brief introduction to MSL data classification.

#### 3.1. Digital elevation models

Data from the Titan were saved in separate files for each channel. The process of georeferencing was carried out simultaneously. It allows for the creation of digital elevation models from all the datasets or else separately for a selected channel. In Fig. 4, digital surface models (DSMs) for three datasets from the Titan channels are presented. The results of the acquisition in SWIR (1550 nm) are quite similar to those from NIR (1064 nm). The most visible dissimilarity is the visible lakebed in the DSM of the G channel (532 nm).

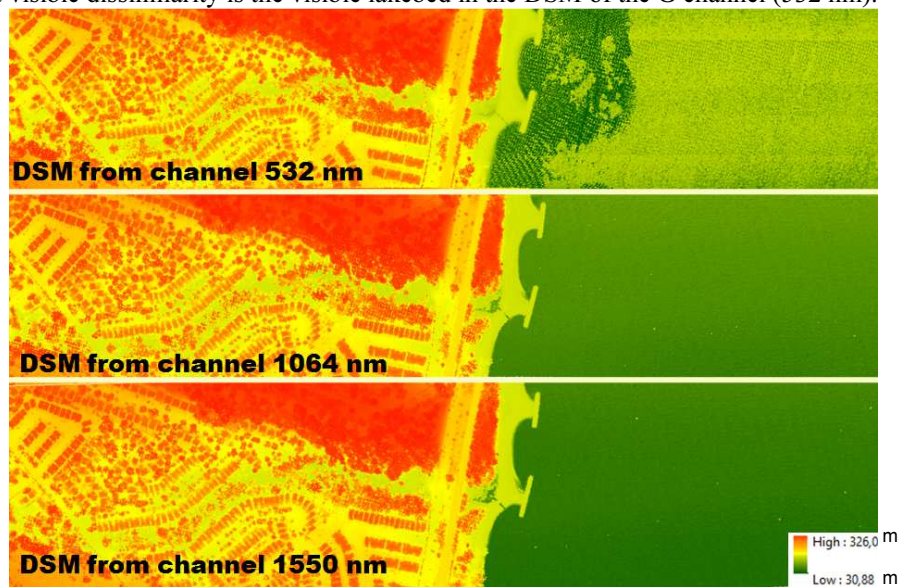


Fig. 4. Comparison of DSMs generated from a point cloud registered with different laser wavelengths by the Titan scanner.

To show the coherence and relative vertical accuracy between point clouds from three bands, differential models from the comparison of two DSMs (Fig. 5) were prepared. Discrepancies for the surface models are also presented in Table 2. When comparing the DSMs, it is apparent that the laser beam of the G channel penetrates the water surface, providing returns from the lakebed. This meant that the mean value of the G band was lower than the mean value of the NIR and SWIR bands: -0.13 m and -0.10 m for the NIR and SWIR bands with respect to the G channel. A fairly high standard deviation (STD) is identified for all the differential models for vegetation areas and buildings' edges. These values are the result of various distributions of points from channels and the high resolution of the DSMs (0.5 m). The results of the comparison of digital terrain models (DTMs) generated from only bare ground points show that there is a much lower shift (less than 0.03 m) between these three DTMs than for DSMs. The mean values for the differential DTMs are close to zero, which means that the point clouds are well adjusted and that they present high relative accuracy. The STD for the DTMs comparison from 0.19 m to 0.27 m is caused by slightly different building classifications in the point clouds from the multi-wavelength laser. The STDs for both the DTMs' and the DSMs' comparison proved that each channel describes land cover objects in a slightly different way. It is worth noting, however, that the merging of the three point clouds from the Titan channels leads to a considerable increase in data density, which positively affects the completeness of the information from the LiDAR data.

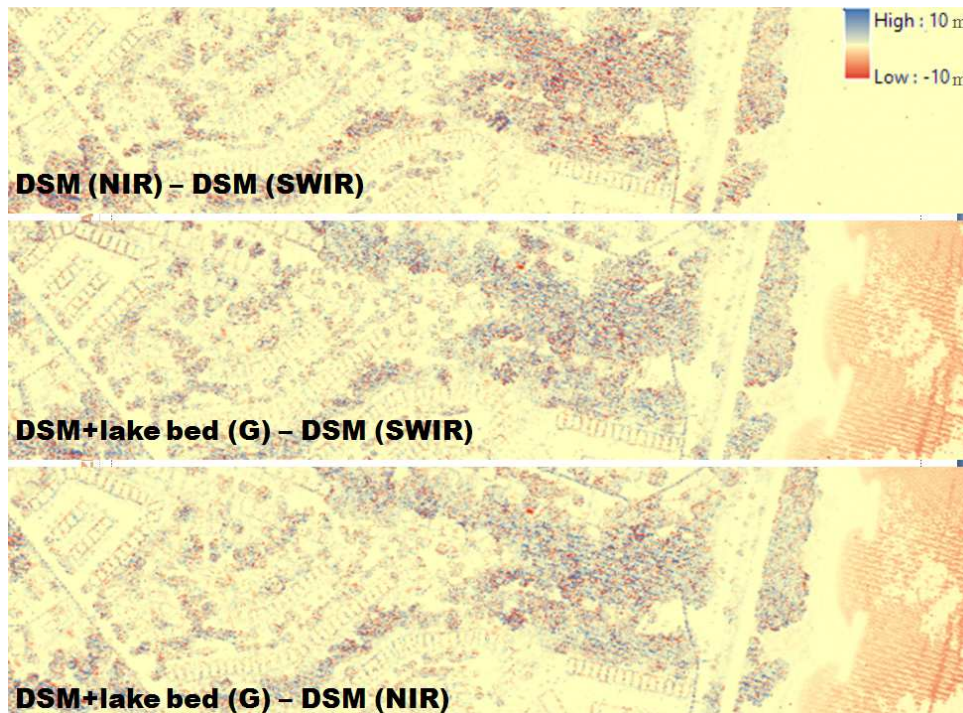


Fig. 5. Differences between the DSMs generated from separated Titan channels.



Tab. 2. Results of the comparison (mean value and STDs) between digital elevation models generated from separated Titan channels (excluding water surface area): difference of the DSMs (upper-right corner); difference of the DTMs (lower-left corner).

Differences MEAN/STD[m]	<b>G</b> 3 <sup>rd</sup> Titan channel	<b>NIR</b> 2 <sup>nd</sup> Titan channel	<b>SWIR</b> 1 <sup>st</sup> Titan channel
<b>G</b> 3 <sup>rd</sup> Titan channel	-	-0.13/2.48	-0.10/2.36
<b>NIR</b> 2 <sup>nd</sup> Titan channel	0.03/0.27	-	0.03/2.48
<b>SWIR</b> 1 <sup>st</sup> Titan channel	0.03/0.21	0.00/0.19	-

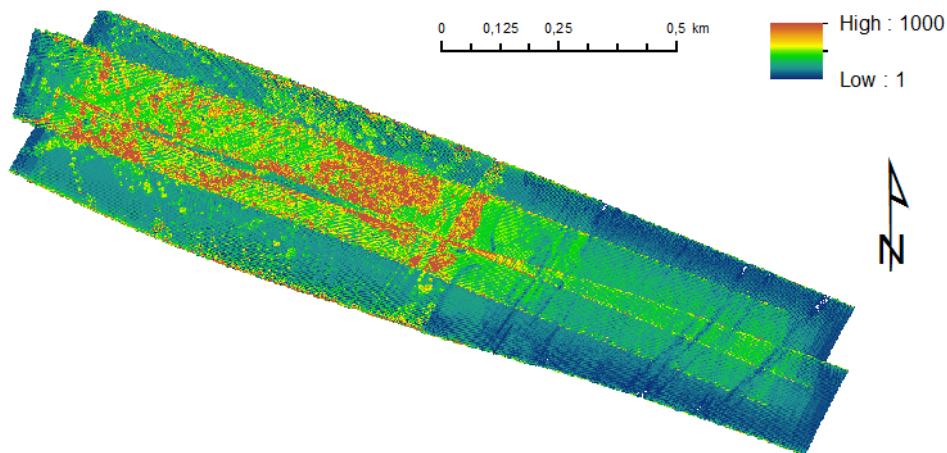


Fig. 6. Density of the point [points/m<sup>2</sup>] cloud collected with the Titan scanner for the test area.

In the case of multispectral ALS, the examined density of the whole point cloud is the sum of the density of the point clouds acquired with three laser wavelengths. It can even be up to several hundred points per square metre in some places; however, the average value of the pulse density for the test area was about 50 points/m<sup>2</sup>, and the average value for the point density was over 60 points/m<sup>2</sup>. These are high values for airborne scanning system, but it should be noticed that the three point clouds are merged here. In Fig. 6, the visualization of the point cloud density for the whole test-study is presented. It can be seen that the land cover (particularly vegetation) has an influence on the density. In the vegetated area, a density of a few points per square metre results from one pulse because of several returns of the laser beam. The influence of the surface water on the decrease in density can also be noticed. Table 3 contains statistics for three point clouds obtained with the multispectral ALS system referring to the classification results, the returns and the densities of the point clouds. As the wavelength scan is lowered, the density of the points increases. This is not just caused by the fact that the number of second and subsequent returns is different: it is less for SWIR (24%) than for NIR (28%) and G (28%). It is also caused by the lower number of points registered on the water surface for SWIR (15%) compared to NIR (20%) and G (28%). This fact also relates to the increasing pulse density for lower wavelengths. The density of the point clouds does not just result from the frequency of the scanner but also from the design of the Titan scanner, which includes a laser emitting at a different angle (7°, 0° and 3.5° for G, NIR and SWIR, respectively).

Tab. 3. Statistics for the classification, returns and density of multispectral ALS data.

<b>Class</b>	<b>G 3<sup>rd</sup> Titan channel</b>	<b>NIR 2<sup>nd</sup> Titan channel</b>	<b>SWIR 1<sup>st</sup> Titan channel</b>
Unassigned	0.02%	0.02%	0.05%
Ground	12.21%	11.23%	9.00%
Low vegetation	10.88%	15.20%	20.79%
Medium vegetation	4.08%	5.41%	6.17%
High vegetation	31.98%	40.09%	39.48%
Building	7.47%	7.62%	9.91%
Noise	0.01%	0.01%	0.00%
Water	27.72%	20.43%	14.60%
Lake bed	5.65%	-	-
<b>Return</b>	<b>G 3<sup>rd</sup> Titan channel</b>	<b>NIR 2<sup>nd</sup> Titan channel</b>	<b>SWIR 1<sup>st</sup> Titan channel</b>
First	73%	72%	76%
Second	19%	17%	16%
Third	6%	8%	6%
Fourth	2%	3%	2%
<b>Density</b>	<b>G 3<sup>rd</sup> Titan channel</b>	<b>NIR 2<sup>nd</sup> Titan channel</b>	<b>SWIR 1<sup>st</sup> Titan channel</b>
Point density	25 p./m <sup>2</sup>	23 p./m <sup>2</sup>	20 p./m <sup>2</sup>
Pulse density	19 p./m <sup>2</sup>	17 p./m <sup>2</sup>	15 p./m <sup>2</sup>
Total number of points	16.3 million	14.0 million	11.8 million

### 3.2. Land cover maps

The data acquisition in three wavelengths provides point clouds with different values for the laser intensity and is related also to the spectral properties of various objects (see Fig. 1). These intensity images are quite different, as shown in Fig. 3. They contain independent information which is confirmed by the correlation matrix presented in Table 4. The correlation coefficient below 0.5 indicates the individual role of each channel in the data acquisition.

Tab. 4. Correlation matrix for the intensity of laser reflectance rasters for channels of the Titan scanner – the values of the radiometric reflectance of the laser beam in a raster with a 0.5 m resolution were used in this calculation.

Correlation coefficients	<b>G</b> 3 <sup>rd</sup> Titan channel	<b>NIR</b> 2 <sup>nd</sup> Titan channel	<b>SWIR</b> 1 <sup>st</sup> Titan channel
<b>G</b> 3 <sup>rd</sup> Titan channel	1.0000	0.34095	0.43500
<b>NIR</b> 2 <sup>nd</sup> Titan channel	0.34095	1.0000	0.41216
<b>SWIR</b> 1 <sup>st</sup> Titan channel	0.43500	0.41216	1.0000

Each acquired point cloud can be orthogonalized to a flat surface in order to create a raster image (an intensity orthoimage). The geometry of such an image resembles a true orthophoto. The ground sampling distance (GSD) of the orthoimages produced from multispectral ALS is dependent on the point cloud density. An approximated density of several points per square metre leads to an intensity image with a GSD no greater than 0.25 m. Such a density is not comparable with orthoimages generated from photogrammetric images with an example GSD of 10 cm for urban areas. On the other hand, such a resolution will frequently be sufficient for land cover mapping, and multispectral ALS used by itself provides more information than RGB values.

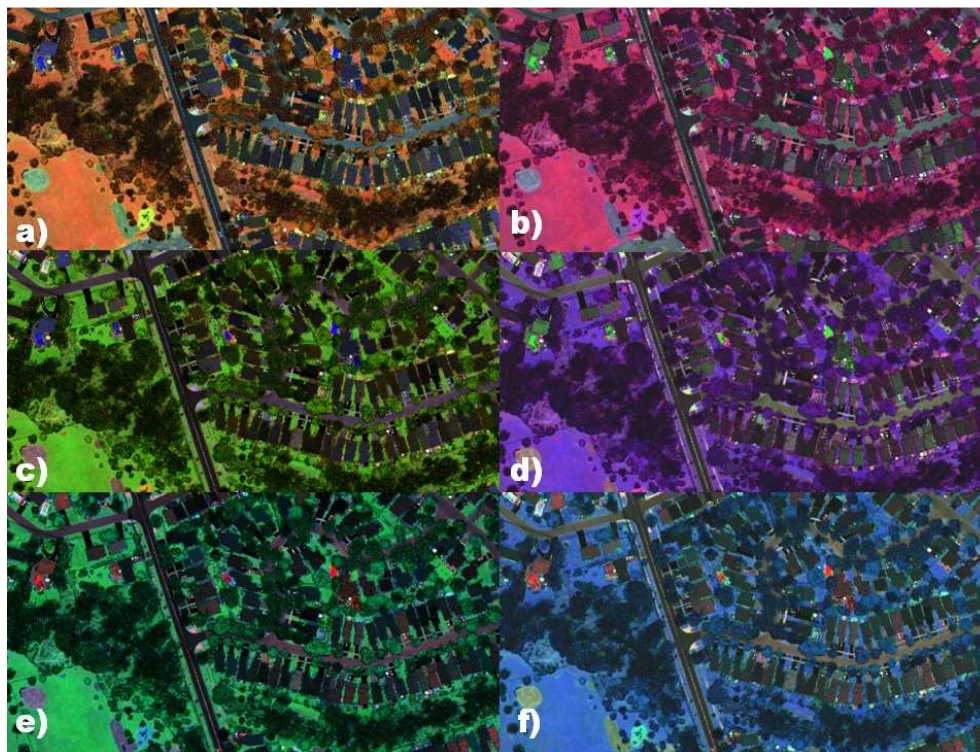


Fig. 7. Six examples of the mapping of multispectral laser scanning data to RGB images: NIR, SWIR, G (a), NIR, G, SWIR (b), SWIR, NIR, G (c), SWIR, G, NIR (d), G, NIR, SWIR (e), G, SWIR, NIR (f).



The above-mentioned laser intensity orthoimages allow for the creation of colour composites. The possibilities for matching the intensity images from three channels to a RGB value of a colour composite are shown in Fig. 7. The colour composites can be generated directly from the corrected intensity images by assigning the intensity values of the three wavelengths to RGB. The properties of the human eye make the best composite when the blue is defined by the reflection in the least-differentiated spectral channel (Fig. 7a and 7c). The use of the G channel for the definition of the red value generates composites with blue and violet dominant that do not provide for a good effect (Fig. 7e and 7f) because the eyes are less sensitive to these colours. If the G channel is used as blue in the generation of the composites, water has an intuitive colour (Fig. 7a and 7c). It should also be noted that the last-mentioned composites are similar to false colour compositions (Fig. 7a) and pseudo-natural colour composites (Fig. 7c) generated from photogrammetric images. In contrast, high vegetation looks different here than in typical false colour and pseudo-natural colour composites. In all the composites that are created from intensity of MSL technology, trees are darker, which is caused by the loss of energy when many returns are registered.



Fig. 8. Shaded DSM overlaid with a colour composition (SWIR, NIR, G (a) and NIR, SWIR, G (b) of multispectral ALS intensity.



Fig. 9. Shaded DSM (the G channel alone) overlaid with colour-coded elevation.



Fig. 10. Shaded DSM (the G channel alone) overlaid with an ALS classification raster (predominant class).

The creation of such colour composites is only possible through acquisition in three spectral bands. This can be achieved by multispectral ALS. Fig. 8 shows the colour composite overlaying the colour-shaded DSM. Such a visualization has the character of



a three-dimensional product which shows land cover in a better way. However, these data can also be visualized in another manner as is typical for ALS data. The land-cover is clearly presented in Fig. 9 and 10, which show a colour-coded elevation and predominant class grid overlaid with a shaded surface model. These forms of visualization show the topography and the land cover and can be obtained by any ALS data.

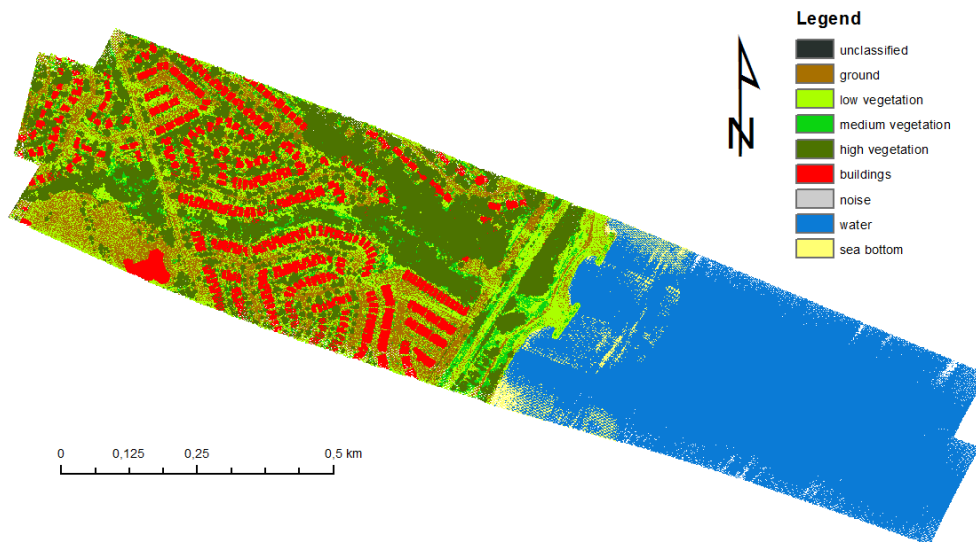


Fig. 11. Raster of the predominant class for the classified data of multispectral ALS.

### 3.3. Data classification

As to the classification of multispectral ALS, two kinds of data processing can be considered. The first type of classification is a typical geometric classification of a LiDAR-based point cloud in which many well-known algorithms are in use, e.g., the TIN active model (Axelsson, 1999) and linear algorithms prediction (Pfeifer *et al.*, 1999), etc. Data acquired with multispectral laser scanning can be classified based on the individual channels or else based on the merged point cloud. The result of the merged point cloud classification processed in Terrasolid software for test data collected with the Titan scanner is shown in Fig. 11. In most approaches to an ALS data classification, the geometric relation of the points or a group of points is taken into account. Meanwhile, a number of software solutions also provide tools to classify points based on the intensity of the laser reflection. The separate classification of the point cloud of every individual spectral channel can provide for classification by the intensity of the reflection.

The second meaning of “classification” referring to multispectral ALS data relates to land cover mapping using the spectral response of different materials and land cover types directly from the LiDAR reflectance values. Height information (i.e., the normalized digital surface model - nDSM) can be used as another band of information to improve such a classification. In this case, the results of the geometric classification of ALS data can also

be used for training areas in order to further improve the classification from multispectral ALS data.

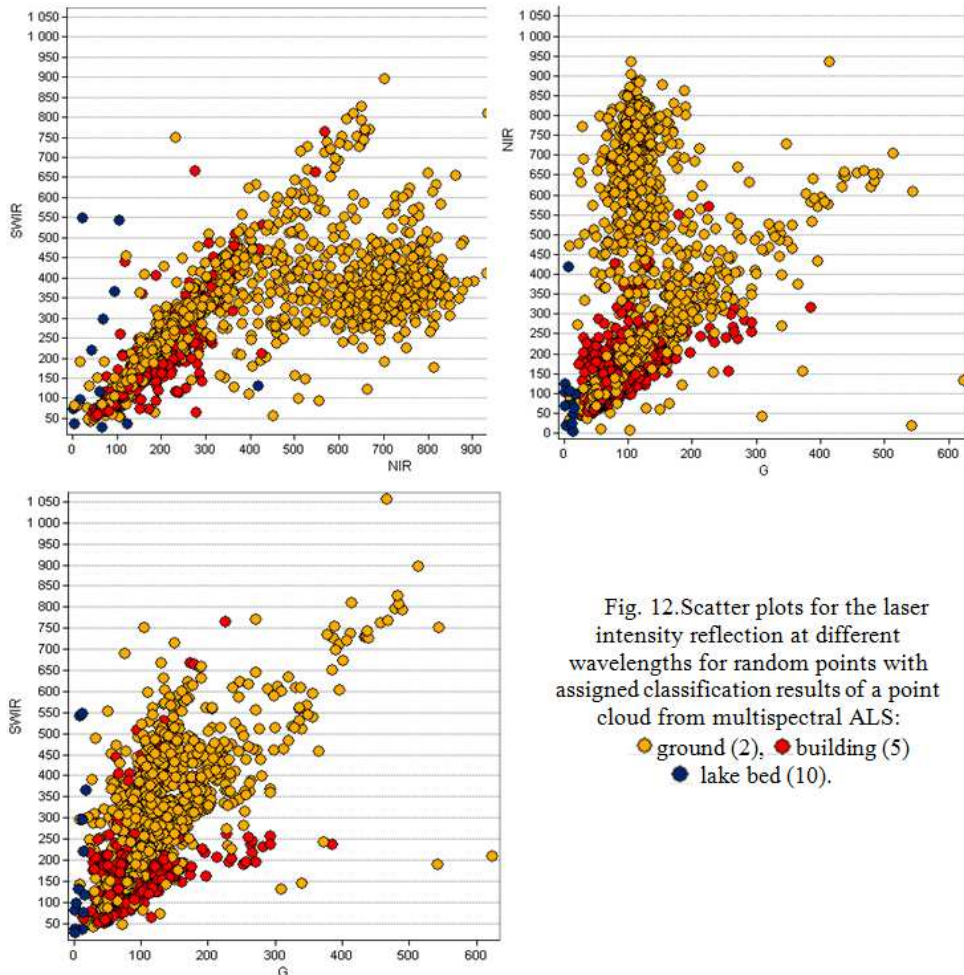


Fig. 12. Scatter plots for the laser intensity reflection at different wavelengths for random points with assigned classification results of a point cloud from multispectral ALS:  
 ● ground (2), ● building (5)  
 ● lake bed (10).

The potential of land cover classification from multispectral ALS data is shown in Figures 12 and 13. Fig. 12 shows the relations between the laser reflectance intensity of the G, NIR and SWIR bands for random cells with predominant classes: the ground, buildings and the lake bed (manually selected from a class of points on water). Intensity values were assigned and scatter plots were prepared for these cells. In this figure, the soil line is clearly visible in the scatter plots of NIR (SWIR) and G (NIR). The distribution of the pixels in these scatter plots presents a shape very similar to the shape seen in a scatter plot presenting the distribution of pixels in a spectral space for passive sensors interpreted as vegetation. This fact can be interpreted in such a way that the point cloud classified as ground was collected as a reflectance of the lowest vegetation, i.e., grass. Both the soil line and the shape that can be linked to vegetation are less visible in relation to G (SWIR). The points classified as buildings are usually assigned lower intensity values in NIR and by using

height information from the ALS data it provides for the possibility of classifying them using just spectral and height information. Cells classified as the lakebed are concentrated where the lowest values of intensity are located.

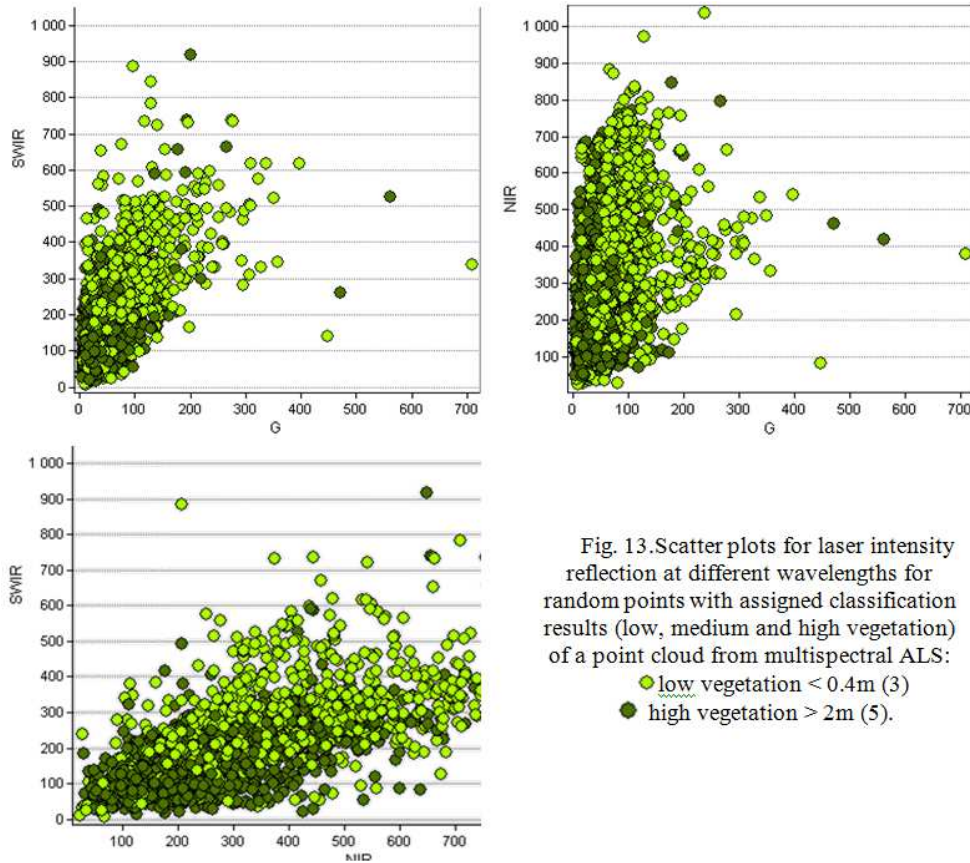


Fig. 13. Scatter plots for laser intensity reflection at different wavelengths for random points with assigned classification results (low, medium and high vegetation) of a point cloud from multispectral ALS:  
 ● low vegetation < 0.4m (3)  
 ● high vegetation > 2m (5).

In Fig. 13, scatter plots for point clouds classified as low, medium and high vegetation are presented. In this case, the distribution of intensity reflectance is more complicated, which can be caused by different species and the different number of returns in vegetation areas. The distribution of spectral information is more balanced here, and only as light relation between height and intensity is visible.

#### 4. DISCUSSION

The use of the laser at different wavelengths is a valuable source of 3D data and information on land cover. The Titan scanner, due to the use of G and NIR lasers, facilitates the integration of topographic and bathymetric data. It is likely that this scanner will frequently be used in environmental case studies, e.g. for national parks and forest districts for vegetation monitoring, because it is an active technique that brings a variety of information about the land cover. Multispectral ALS will also be used in archaeology,

which has already been proven by Briese *et al.* (2013), showing an application of colour compositions from intensity orthoimages. In many cases, the Titan may be used for both topographic and bathymetric scanning, providing 3D data with a density higher than normal scanners, as was demonstrated in the presented analysis. This sensor can also be very valuable for hard-to-reach areas for which airborne data are only in frequently acquired. It is probable that, in the long term, the Titan scanner might be used to automatically create land cover maps, which is the greatest advantage of this sensor in the designer's opinion. However, this objective can only be achieved when sufficient classification algorithms combining elevation information and intensity values are used. The presented scatter plots demonstrated a problem with the separation of the selected classes, especially vegetation of different heights.

Multispectral scanners – and despite that the Titan is at present a unique sensor -will not replace regular topographic ALS and financed photogrammetric flight missions (particularly those by governmental units), which are used for typical elevation models from ALS and orthophotomaps in colour and false colour composites. Photogrammetric orthoimages and even true orthoimages resulting from an orthogonalized point cloud generated with dense image matching exceed colour composites for the intensity of multispectral ALS with respect to the spatial resolution.

The presented analysis and figures show the potential of multispectral ALS, beginning with the provision of information about the height and geometry of objects, and ending with the creation of colour orthophotos from the intensity of the laser beam and land cover map. These data also allow the LiDAR point clouds to be colourized instead of using aerial images for assigning RGB values to each point, as is typical for ALS processing, and such a colour point cloud would have a completely different look.

## **5. CONCLUSION AND POSSIBLE FUTURE WORK**

The Titan scanner (by Optech) is undoubtedly a new opportunity for airborne LiDAR technology. It is a tool for high-density topographic surveying which can be useful for land cover classification and shallow water bathymetry. It can provide for a wide range of possibilities in natural and archaeological applications. It can be an alternative or else a supplement for photogrammetric data collection.

Future work with this kind of data should be related to the development of the classification of point clouds using both geometric relations and information about the intensity from multispectral acquisitions. There is a need for investigation that shows how multispectral ALS can supplement photogrammetric data. Finally, tools for multispectral ALS data processing should differ slightly from the typical, particularly when options related to intensity correction and colourizing point clouds are concerned. It is expected that, in the next few years, the subject of multispectral ALS will become one of the new trends in LiDAR technology.

## **6. ACKNOWLEDGEMENTS**

I would like to thank Optech Inc. for providing the data from the Titan scanner. I would particularly like to offer my thanks to Mr Michael Zarzeczny for the presentation of the Titan system.

## LITERATURE

- Axelsson P., 1999. Processing of laser scanner data – algorithms and applications. *ISPRS, Journal of Photogrammetry & Remote Sensing*, 54, pp. 138-147.
- Briese C., Pfennigbauer M., Ullrich A., Doneus M., 2013. Multi-wavelength airborne laser scanning for archaeological prospection. *International Archives of Photogrammetry, Remote Sensing and Spatial Information Science*, 40, pp. 119-124.
- Chust G., Galparsoro I., Borja Á., Franco J., Uriarte A., 2008. Coastal and estuarine habitat mapping, using LIDAR height and intensity and multi-spectral imagery, *Estuarine, Coastal and Shelf Science*, 78(4), pp. 633–643.
- Doneus M., Miholjek I., Mandlbürger G., Doneus N., Verhoeven G., Briese C., Pregesbauer M., 2015. Airborne laser bathymetry for documentation of submerged archaeological sites in shallow water. *International Archives of Photogrammetry, Remote Sensing and Spatial Information Science*, 1, pp. 99-107.
- Elsayed K. A., Chen S., Petway L. B., Meadows B. L., Marsh W. D., Edwards W. C., Barnes J. C., DeYoung R. J., 2002. High-energy, efficient, 30-Hz ultraviolet laser sources for airborne ozone-lidar systems. *Applied optics*, 41(15), pp. 2734-2739.
- Gong W., Sun J., Shi S., Yang J., Du L., Zhu B., Song S., 2015. Investigating the Potential of Using the Spatial and Spectral Information of Multispectral LiDAR for Object Classification. *Sensors*, 15(9), pp. 21989-22002.
- Lang M. W., McCarty G. W., 2009. Lidar intensity for improved detection of inundation below the forest canopy. *Wetlands*, 29(4), pp. 1166-1178
- Morsdorf F., Nichol C., Malthus T., Woodhouse I. H., 2009. Assessing forest structural and physiological information content of multi-spectral LiDAR waveforms by radiative transfer modelling. *Remote Sensing of Environment*, 113(10), pp. 2152-2163.
- Mierczyk Z., Zygmunt M., Kaszczuk M., Muzal M., 2013. Multispectral Laser Head for Terrain Identification and Analysis. *Acta Physica Polonica*, 124(3), pp. 502-504.
- Pfeifer N., Reiter T., Briese C., Rieger, W., 1999. Interpolation of high quality ground models from laser scanner data in forested areas. *International Archives of Photogrammetry and Remote Sensing*, 32(3/W14), pp. 31-36.
- Pfennigbauer M., Ullrich A., 2011. Multi-wavelength airborne laser scanning. Proceedings of the International Lidar Mapping Forum, ILMF, New Orleans.
- van Rees, E. (2015). The First Multispectral Airborne Lidar Sensor. *GeoInformatics*, 18(1), pp. 10-12.
- Shi S., Song S., Gong W., Du L., Zhu B., Huang X., 2015. Improving Backscatter Intensity Calibration for Multispectral LiDAR. *IEEE Geoscience and Remote Sensing Letters*, 12(7), pp. 1421-1425.
- Suomalainen J., Hakala T., Kaartinen H., Raikonen E., Kaasalainen S., 2011. Demonstration of a virtual active hyperspectral lidar in automated point cloud classification. *ISPRS Journal of Photogrammetry*, 66, pp. 637–641.



Vain A., Yu X., Kaasalainen S., Hyypä J., 2010. Correcting Airborne Laser Scanning Intensity Data for Automatic Gain Control Effect. *IEEE Geoscience and Remote Sensing Letters*, 7(3), pp. 511 - 514.

Vain A., Kaasalainen S., Pyysalo U., Krooks A., Litkey P., 2009. Use of Naturally Available Reference Targets to Calibrate Airborne Laser Scanning Intensity Data. *Sensors*, 9(4), pp. 2780-2796.

Wallace A., Nichol C., Woodhouse I., 2012. Recovery of Forest Canopy Parameters by Inversion of Multispectral LiDAR Data, *Remote Sensing*, 4(2), pp. 509-531.

Wang C., Glenn, N. F., 2009. Integrating LiDAR intensity and elevation data for terrain characterization in a forested area. *IEEE Geoscience and Remote Sensing Letters*, 6(3), pp. 463-466.

Wichmann V., Bremer M., Lindenberger J., Rutzinger M., Georges C., Petrini-Monteferrri F., 2015. Evaluating the potential of multispectral airborne LiDAR for topographic mapping and land cover classification. *ISPRS Annals of the Photogrammetry, Remote Sensing and Spatial Information Sciences*, 1, 113-119.

## MULTISPEKTRALNE LOTNICZE SKANOWANIE LASEROWE - NOWY TREND W ROZWOJU TECHNOLOGII LIDAR

SŁOWA KLUCZOWE: multispektralne lotnicze skanowanie laserowe, długość fali lasera, rozwój technologii, klasyfikacja, kompozycja barwna, mapa pokrycia terenu

### Streszczenie

Jedną z najbardziej dokładnych technologii pozyskiwania danych o terenie i jego pokryciu jest lotnicze skanowanie laserowe (ALS). W wieloletnim rozwoju skanerów laserowych dążono przez lata do osiągnięcia jak najwyższej dokładności pomiaru oraz jak największej gęstości danych, co związane było przede wszystkim z jakością danych i kosztami pracy. Obecnie istnieje kilka możliwości dalszego rozwoju tego typu systemów, wśród których wymienić należy zwiększanie zasięgu skanowania laserowego, a także rejestracja odbić w kilku zakresach spektralnych. Szczególnie ostatni trend w rozwoju technologii LIDAR pozwala na inne spojrzenie na dane w postaci chmur punktów, które jeszcze efektywniej mogą tworzyć mapy pokrycia terenu niż typowe lotnicze skanowanie topograficzne (ALS).

W rozwoju lotniczego skanowania laserowego istotnym krokiem było pojawienie się lotniczego skanowania hydrograficznego (batymetrycznego). W różnych rozwiązaniach producentów, pojawił się laser o częstotliwości odpowiadającej zakresowi w paśmie zielonym światła widzialnego. Przy rejestracji intensywności zaobserwowanych podczas skanowania różnymi skanerami laserem o różnej długości fali dla tego samego obszaru, dostrzeżono różne właściwości refleksyjnymi obiektów analogiczne do rejestracji w różnych zakresach spektralnych technikami pasywnymi. Sprawilo to, że w ostatnich latach pojawiły się pierwsze systemy skanowania lotniczego wykorzystujące więcej niż 2 zakresy spektralne w jednym skanerze. Od tego czasu można zatem mówić o multispektralnym lotniczym skanowaniu laserowym. Rejestracja chmur punktów w 3 zakresach spektralnych pozwala poza zapisem współrzędnych i innych atrybutów charakterystycznych dla skanowania topograficznego, na zapis również 3 wartości intensywności odbicia, co umożliwia tworzenie kompozycji barwnych w postaci true-orto obrazów.

W artykule zaprezentowano przykładowy system multispektralnego lotniczego skanowania laserowego wraz z możliwościami, jakie dają dane nim pozyskane, poruszając kwestię gęstości danych, dokładności numerycznych modeli wysokościowych z nich tworzonych. W wyniku analiz udowodniono wysoką dokładność wzajemną rejestracji w poszczególnych kanałach spektralnych wynoszącą do 0.03 m. W analizie gęstości danych ukazano wpływ długości fali na gęstość chmury punktów. Rozpatrywana chmura punktów miała średnią gęstość 25, 23 i 20 punktów na metr kwadratowy odpowiednio dla lasera z zakresu pasma zielonego, bliskiej podczerwieni i średniej podczerwieni. W artykule poruszono także problematykę tworzenia kompozycji barwnych ortobrazów z intensywności odbicia oraz możliwości klasyfikacji ich treści. W referacie poddano również dyskusji możliwość zastosowania danych z multispektralnego lotniczego skanowania laserowego w tworzeniu map pokrycia terenu w porównaniu z tradycyjnymi technikami fotogrametrycznymi.

Dane autora:

Dr inż. Krzysztof Bakula  
e-mail: k.bakula@gik.pw.edu.pl  
telefon: 22 234 7587

Przesłano 9.11.2015  
Zaakceptowano 20.12.2015